TRABAJO FIN DE MASTER

Prevalence of *TERT* promoter mutations in Anaplastic Thyroid Carcinomas. Concurrent activation of *TERT* and MAPK signalling pathway.

Realizado por
Mª Ángeles Rodríguez García
Dirigido por
Dra. Ginesa García-Rostán Pérez

Septiembre 2018

INDEX

Introduction

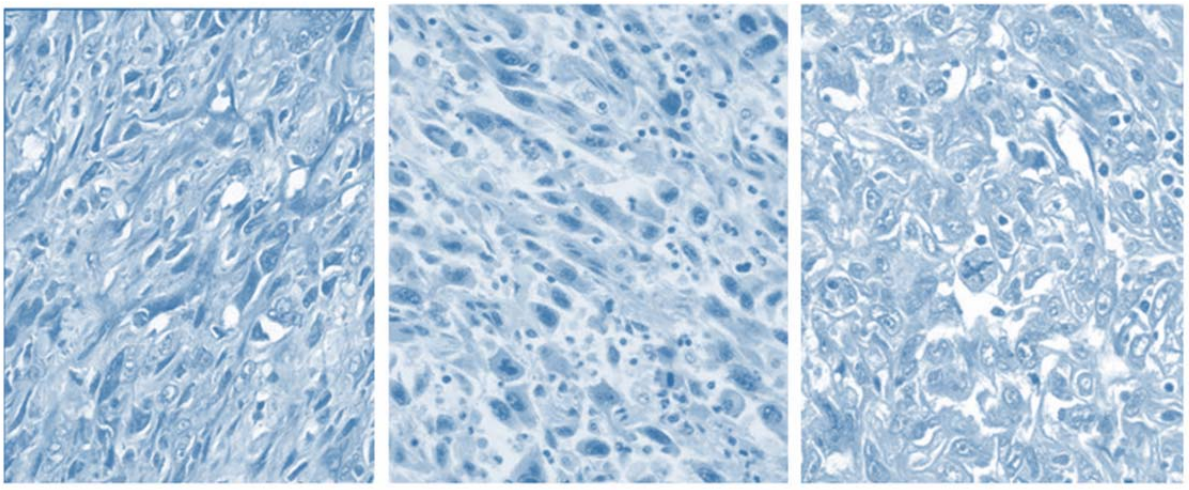

1. Cancer and Oncogenesis

As it is known, cancer is defined as an uncontrolled growth of cells in a located part of the body. The problem starts when, from a normal division of cells, an alteration occurs that provokes this abnormal growth, and ends in a mass of cells (Tumour). It can occur that the system acts repairing this situation, by causing apoptosis in those transformed cells, so they would die. However, in case the damage cannot be repaired, they would keep on growing and invading other organs or tissues leading to local or distant metastasis [Figure-1]. [1]

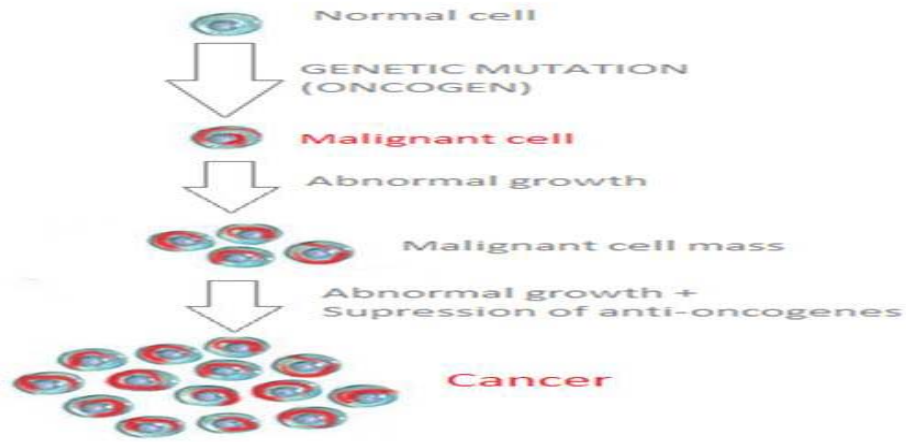

One responsible mechanism for cancer is known as **oncogenesis,** in which cancer process is characterized by genetic changes at cellular levels. Genes do affect and control the way our cells function, concretely how they divide and growth. **Oncogenes** are those particular genes that result from somatic mutations or changes, causing alterations in the normal control of cell division and cell growth. [2]

2. Thyroid Gland

The thyroid gland is below the thyroid cartilage (also known as Adam's apple) in the front part of the neck. It is butterfly shaped, with 2 lobes joined by a narrow isthmus. Thyroid gland normally produces thyroid hormone, which is important to the normal regulation of the metabolism of the body and is formed by 2 main types of cells: Follicular and Parafollicular cells or C Cells.

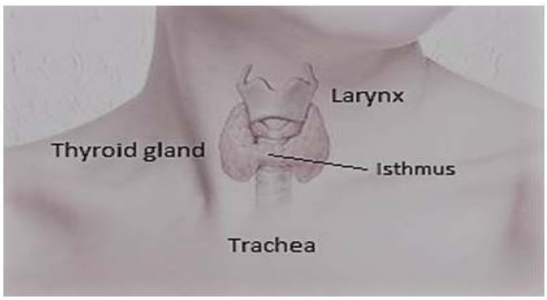

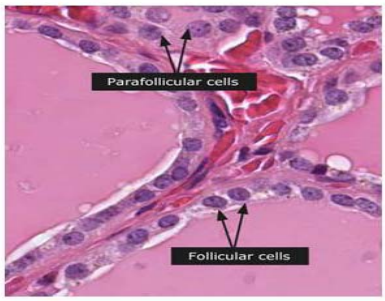

This gland produces and releases two hormones, called triiodothyronine ($\mathbf{T_3}$) and thyroxine ($\mathbf{T_4}$). They are tyrosine-based hormones responsible for regulation of metabolism and part of the endocrine system. Both, T_3 and T_4, are partially composed of iodine and both are regulated by the hypothalamus in the brain. [3]

3. Thyroid Cancer

Thyroid cancer is the most common type of endocrine malignancy with an incidence that has steadily increased during the past decades. In the past 15 years its incidence is increasing at a much faster rate than in any other cancer type. Affects women more often than men, and usually occurs in people between 25 and 65 years. [4]

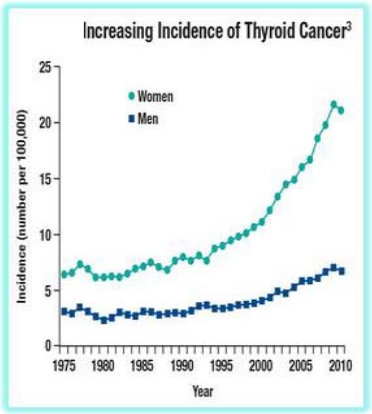

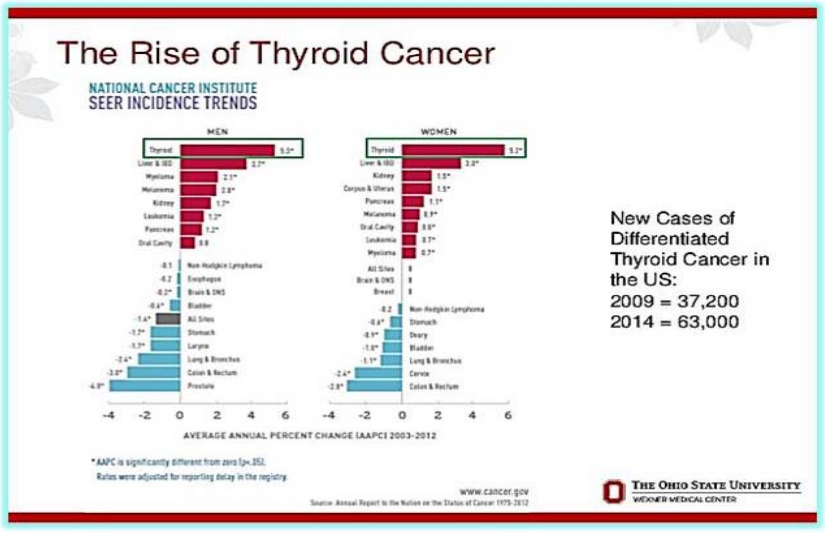

Because thyroid is a radiosensitive organ, radiation exposure is also associated with a high risk of thyroid cancer, especially in children. [5]

3.1 Histological Classification of Thyroid Cancer

Malignant cancers of the thyroid arise from two different types of parenchymal cells: Follicular and Parafollicular cells or C Cells

- **Follicular cells** wrap the follicles filled with colloid, concentrate iodine and synthesize thyroid hormones. From these cells arise well differentiated, poorly differentiated and **anaplastic thyroid cancers (ATCs),** the main aim of this study.
- **Parafollicular** or **C cells** are spread among the thyroid follicles and synthesize calcitonin. From these cells arise medullary thyroid carcinomas, which represent only 3% of thyroid cancers

➢ Follicular Cell derived Thyroid Cancers:

Well differentiated thyroid carcinomas (also called **DTCs**) account for around 90% of all thyroid cancers, while poorly differentiated carcinomas (**PDCs**) represent 7% and anaplastic carcinomas (**ATCs**) 5%.

Overall, DTCs have a very good prognosis with a long term disease free survival close to 95% in papillary thyroid carcinomas (**PTC**), 80% in minimally invasive follicular thyroid carcinomas (**mi-FTC**) and 50% in widely invasive follicular thyroid carcinomas (**wi-FTC**). Their treatment is based on a studied approach that includes thyroidectomy, radioactive iodine therapy and hormonal suppression (TSH) with thyroid replacement hormone.

- **Papillary Thyroid Carcinoma (PTC)** is the most common type of thyroid cancer. **PTCs** are slow growing, differentiated cancers that can develop in one or both lobes of the thyroid gland. They usually spread to nearby lymph nodes in the neck. [6]

- **Follicular Thyroid Carcinoma (FTC)** is the second most common type of thyroid cancer. It is found more frequently in countries with an inadequate dietary iodine intake. **FTCs** do not usually spread to nearby lymph nodes, they spread to other organs like the lungs or the bones, more likely than **PTC**. [6]
- **Poorly Differentiated Thyroid Carcinoma** (**PDC**) is a malignant neoplasm of follicular cell origin showing intermediate histopathological patterns between differentiated and undifferentiated thyroid carcinomas. [6]
- **Anaplastic Thyroid Carcinoma** (**ATC**) is the most undifferentiated type of thyroid cancer, meaning that it looks the least like normal cells of the thyroid gland. Though **ATCs** do not express markers of thyroid differentiation such as Tg, TTF1, TPO, keep the expression of epithelial markers (e.g Low molecular weight cytokeratins). It is a very aggressive form of cancer that quickly spreads to other parts of the neck and body. [6-10]

The following figure shows the stepwise progression of follicular cell derived neoplasms

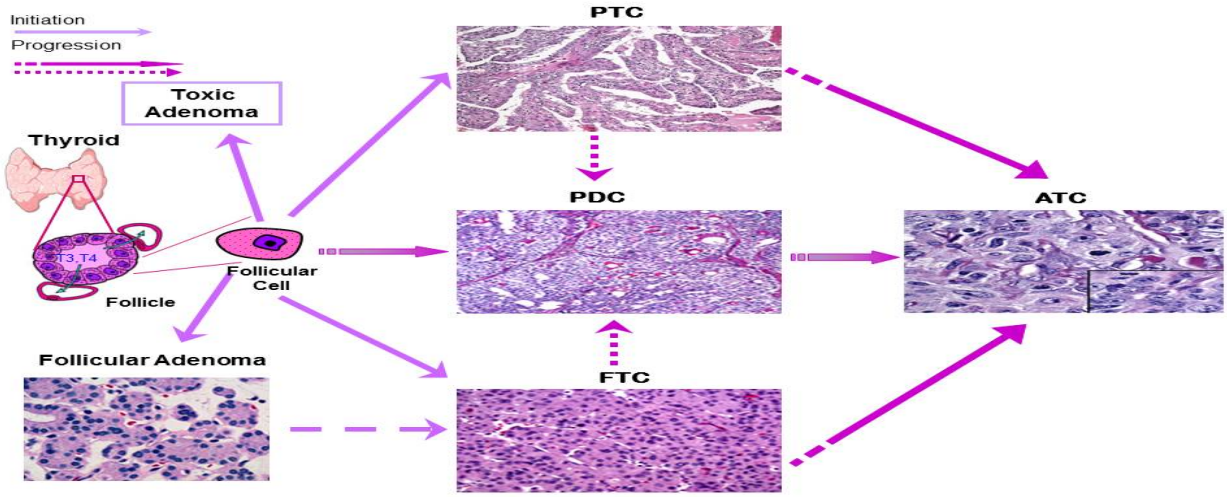

As illustrated in the figure above **ATCs** may arise *de novo* or by dedifferentiation of prior well-differentiated carcinomas (**PTC** or **FTC**) or poorly differentiated thyroid carcinomas (**PDCs**). Morphologically can be subdivided in 4 types: *sarcomatoid*, *epithelioid*, squamous *and small cell type*.

ATCs are extremely aggressive, fast growing tumors, with a dismal prognosis. Most patients died within the first 6-9 months of diagnosis. [7-10]

4. TERT (Telomerase reverse transcriptase)

Telomerase Reverse Transcriptase, also abbreviated as **TERT**, is the catalytic subunit of the enzyme telomerase which, together with the telomerase RNA component (TERC), comprises the most important unit of the telomerase complex. The telomerase enzyme consists of two major components that work together:

- The hTERT or TERT component produced by the *TERT* gene
- The hTR component produced by the *TERC* gene.

The hTR component provides a template for creating the repeated sequence of DNA that telomerase adds to the ends of chromosomes, whilst the TERT component adds the new DNA segment to chromosome ends. They are considered the ribonucleic component and the proteic component, respectively. [11]

The Telomerase Reverse Transcriptase has an essential role in telomere maintenance and cancer biology.

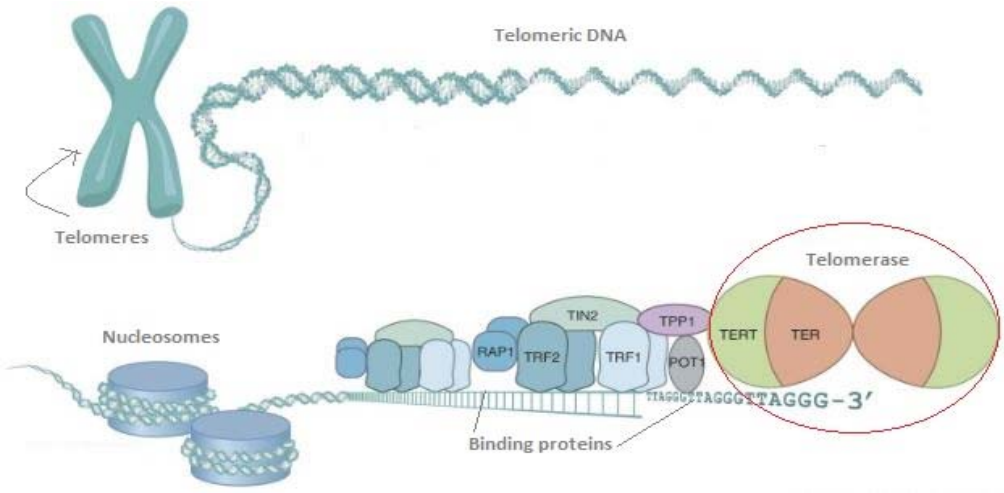

Telomere structure and telomerase recruitment. Adapted from Telomerase Structure, Sandin, S. & Rhodes, D.

5. TERT's role in cancer

Telomerases are part of a distinct subgroup of RNA-dependent polymerases. They lengthen telomeres allowing senescent cells that otherwise would undergo apoptosis to exceed the Hayflick limit* and become potentially immortal, as is often the case in cancerous cells.

*The Hayflick limit or Hayflick phenomenon is the number of times a normal human cell population will divide before cell division stops.

Deregulation of telomerase expression in somatic cells has been involved in oncogenesis. The enzyme complex acts through the addition of telomeric repeats (TTAGGG) to the ends of chromosomal DNA. This generates *immortal cancer cells.* [12]

The best explanation for this is that, as known, telomeres protect chromosomes from abnormally sticking together or breaking down. In most cells, telomeres become progressively shorter as the cell divides. After a certain number of cell divisions, the telomeres become so short that they trigger the cell to stop dividing or to self-destruct (undergo apoptosis). Telomerase counteracts the shortening of telomeres by adding small repeated segments of DNA (TTAGGG) to the ends of chromosomes each time the cell divides.

In most types of cells, telomerase is either undetectable or active at very low levels, but telomerase is abnormally active in most cancer cells, which grow and divide without control or order.

In fact, there is a strong correlation between telomerase activity and malignant tumors or cancerous cell lines. [13] Approximately 90% of cancers disclose increased telomerase activity. Lung cancer is the most well characterized type of cancer associated with increased telomerase expression, but also thyroid cancer displays increased expression of telomerase.

It has been shown that the two commonest mutations reported within the ***TERT*** promoter (**C228T** and **C250T**) generate new binding CCGGAA/T motifs for transcription factors of the family Ets/TCF, leading to increased **TERT** expression

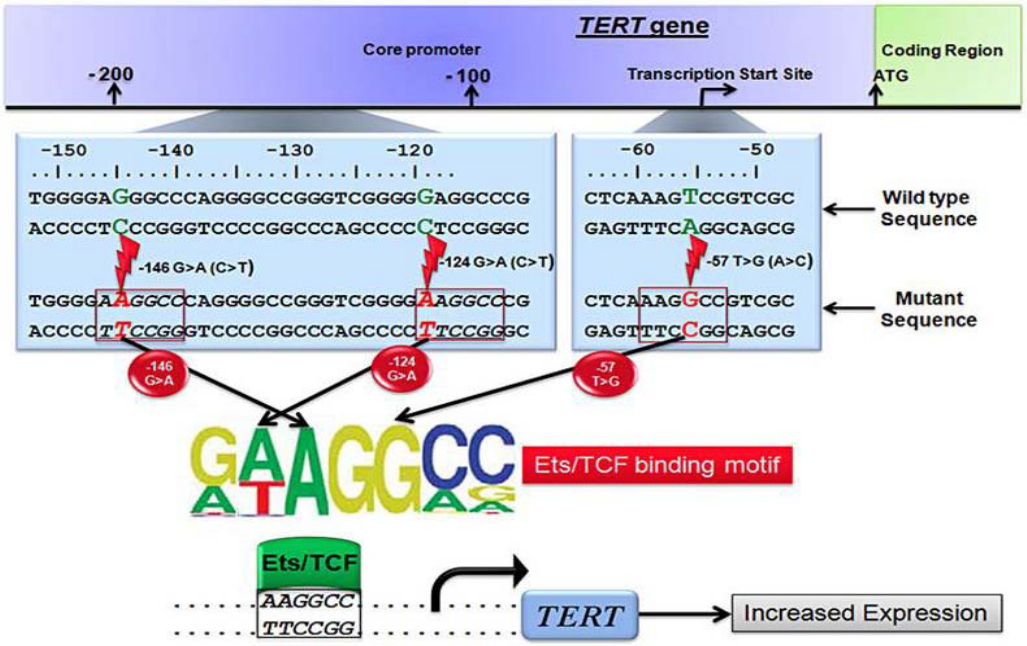

Adapted from Hermminki – Molecular Genetic Epidemiology

Different histotypes of thyroid cancer have been reported to harbour the two main recurrent mutations found in various human cancer types (c.1-124 C<T and c.1-146 C>T). Mutation rate seems to increase with tumor de-differentiation. There are, however, few studies in **ATCs** and most of them include very few cases because it is not easy to recruit **ATCs** to investigate with.

Objectives

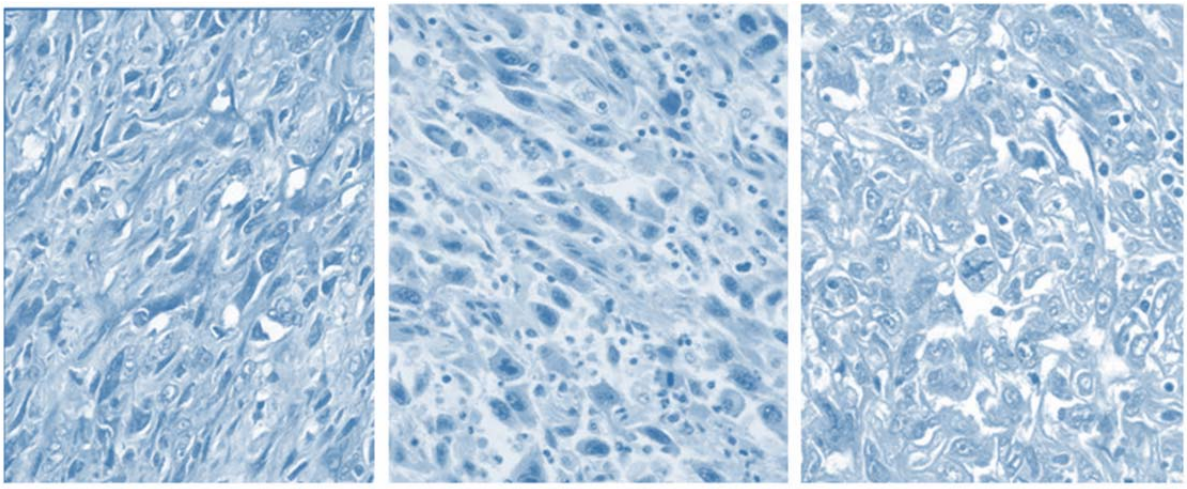

IN THIS STUDY, WE SEEK TO DETERMINE:

1. **THE PREVALENCE OF *TERT* PROMOTER MUTATIONS IN A SMALL SERIES OF ATCs.**

2. **THE CLONAL OR SUBCLONAL NATURE OF *TERT* PROMOTER MUTATIONS.**

3. **THE PRESENCE OR ABSENCE OF *TERT* PROMOTER MUTATIONS IN CONCURRENT BETTER DIFFERENTIATED AREAS GENOTYPED WITHIN THE SAME TUMOR.**

4. **THE SEGREGATION OR NOT OF *TERT* PROMOTER MUTATIONS WITH METASTATIC CELLS TO LOCAL AND/OR DISTANT SITES.**

5. **THE ASSOCIATION OR NOT OF *TERT* PROMOTER MUTATIONS WITH ESTABLISHED ONCOGENIC EVENTS IN ATCs (e.g. mutations in *BRAF* and *RAS*, and *PIK3CA*)**

Materials and Methods

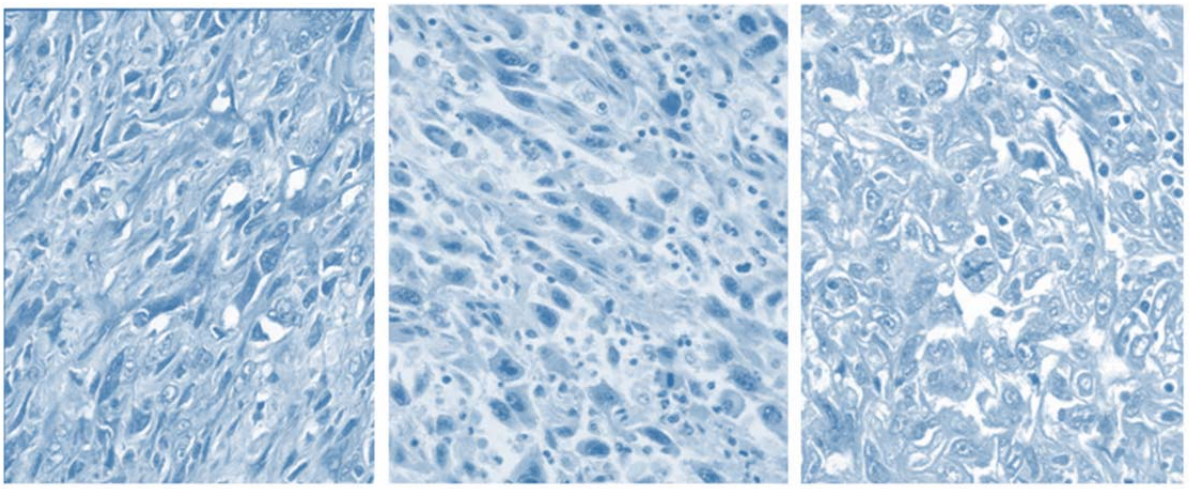

1. Material:

The study encompasses 23 different tumour samples / specimens from a cohort of 9 randomly selected patients who underwent surgery for **ATC**.

ATCs were collected from the files of Pathology Departments of several Hospitals. All of the patients underwent the same protocols of surgical and medical treatment.

Patient information was obtained from review of the patient´s charts. For each case, sex and age at diagnosis, tumor size, histological subtype, presence of extrathyroidal extension, presence of vascular invasion, presence of lymph node and/or distant metastases, stage and follow up were recorded. Tumors were staged according to the recommendations of the International Union Against Cancer (UICC). All processing of clinical information and materials proceeded in accordance with review board approved protocols

All diagnoses were reviewed according to established morphological criteria. Areas of concurrent better-differentiated thyroid carcinoma foci, areas with different microscopic appearance (e.g. spindle / sarcomatoid like or giant cell / epitheliod pattern of growth within the same ATC) but the same histological grade, recurrences, and/or lymph node / distant metastases have been separately analysed.

2. Methods:

2.1 DNA extraction

Hematoxilyn-eosin stained sections cut from each of the 23 paraffin-embedded tumor specimens were microscopically examined to determine the percentage of tumor cells comprising the lesions. Though most of the tissue sections contained only tumor tissue, some included non tumoral thyroid follicles entrapped within the tumor, areas of necrosis or coexisting better differentiated tumor areas. In all the latter cases manual microdisecction was performed to avoid as much as possible degraded DNA and achieve at least 90-95% of tumor purity. A better differentiated component within the ATC tumor (either a PDC or PTC area) was separately genotyped in 67% of the cases. Likewise, areas with different microscopic appearance within the ATC tumor (e.g. squamoid, sarcomatoid / spindle cell, small cell and epitheliod morphology) were separately characterized in 2 cases

Samples were cut with a Microtome HM355S, from *Thermo Fisher Scientific*. The amount of tissue cut to obtain enough DNA to work with varied in function of the size of the tumor biopsy and cellularity of each sample (average 50-120µm). Once cut, tissue sections were subjected to deparaffinization with Xylene at 65ªC followed by hydratation in two steps, first with ethanol 80% + xylene 20% and second with ethanol 100%. It is important to leave the sample completely dry at room temperature before proceeding with DNA extraction

To extract the DNA samples were processed with a commercial kit “GeneJET FFPE DNA purification Kit” (*Thermo Scentific*). Briefly, the protocol has the following steps:

1) Washing with 200ul digestion Buffer provided with the kit during 3 min at 90ºC to eliminate any debris of paraffin that could remain in the tissue

2) Incubation with Digestion and proteinase K in rotation at 65ºC the necessary time to effectively disintegrate the tissue and completely digest the proteins present in the substrate. In our case, samples were on average 3 days on digestion adding if required some extra Proteinase K to favour the process. Sample must be absolutely translucent before proceeding with the following step.

3) Heating of sample at 90ºC during 40 min to eliminate the chemical cross-linking of proteins caused by formaldehyde fixation of tissues in Pathology Departments.

4) Enzymatic digestion of RNA present in the sample with 10ul of RNAase. Sample must be left at room temperature for 10 min and mixed thoroughly. RNA that in case of being present will be eliminated in a later washing step.

5) Transfer of the sample, homogenously mixed with 200ul of Binding Buffer provided with the kit, to the column. The Binding buffer will promote the attachment of the DNA present in the sample to the membrane existing in the column.

6) Washing of the DNA attached to the membrane with 500ul of two consecutive solutions provided with the kit and named buffer 1 and buffer 2. The objective is to eliminate with solutions formulated mainly with ethanol any contaminants present within the sample (RNA, proteins,…..)

7) Transfer of the purification column to the final, sterile, 1.5 ml collection tube and elution of the entrapped DNA with the elution buffer provided with the kit, which consists basically of water free of nucleases. To recover the maximum of DNA adhered to the membrane we perform a second elution with less volume in a different 1.5 ml tube

2.2 DNA quantification and Quality assessment

Before using in any experiment the DNA extracted, it is necessary to know its concentration, purity and quality. All the DNAs used in the study were evaluated first by spectrophotometric analysis in a NanoDrop and then by agarose gel electrophoresis

2.2.1 Spectrophotometric Analysis

Though spectrophotometric analysis is probably the most widespread technique for measuring DNA concentration and DNA purity, formalin-fixed tissue samples with important protein crosslinking are difficult to evaluate spectrophotometrically leading to low throughput DNA quantitation

This step was approached in the NanoDrop 2000c, from *Thermo Fisher Scientific*. The ultraviolet absorbance ratio at 260/280 allows us to asses putative contaminations by proteins and detects the presence of RNA. The ultraviolet absorbance ratio at 260/230 enables us to know if there are salts in the sample that may seriously interfere in ulterior experiments. To assure that each quantitation is correct, the NanoDrop pedestal is carefully washed with water before and after each measurement. Both DNA elutions are quantified on each case (see **Figure 7**)

Figure 7 shows the results obtained in the quantification of 5 DNA samples. The first column is for sample identification. In our case named TNT 8 to 11. The second column measures the *concentration* of DNA in ng/µL in two consecutive measures. The average between the two measurements is calculated. The following columns are for the ultraviolet absorbance ratios at 260nm and 280nm. The handwriting column indicates the dilution chosen to obtain at least 20 ng/µL of DNA for PCR amplification.

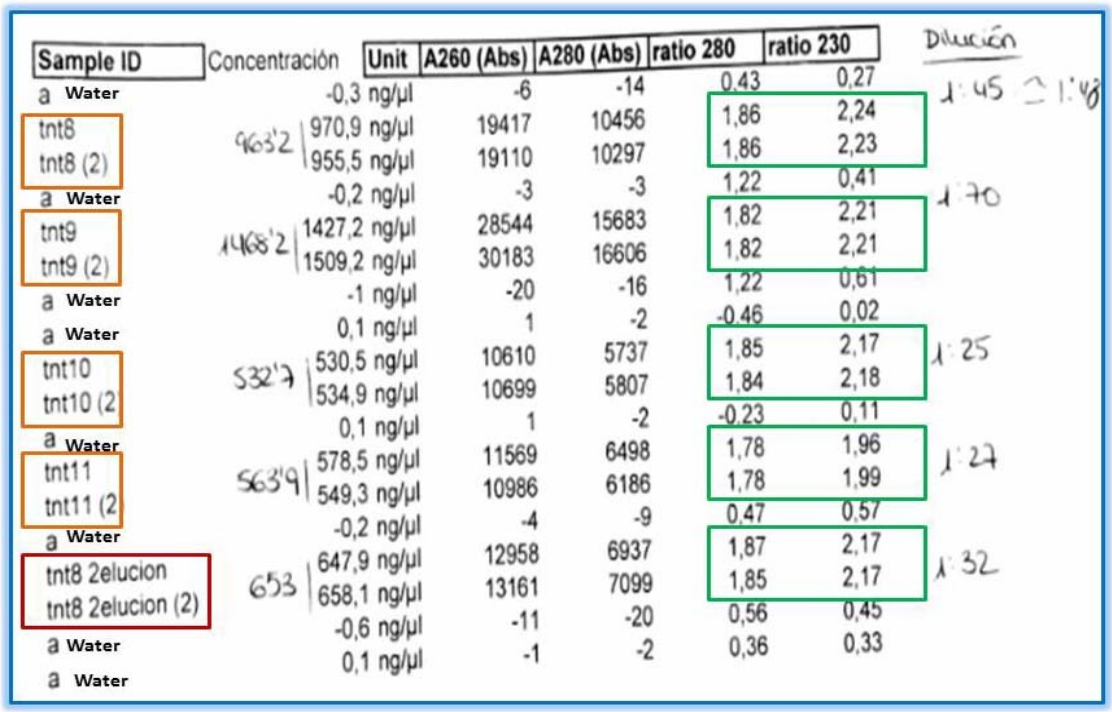

Sample ID	Concentración	Unit	A260 (Abs)	A280 (Abs)	ratio 280	ratio 230	Dilución
a Water		-0,3 ng/µl	-6	-14	0,43	0,27	
tnt8	9632	970,9 ng/µl	19417	10456	1,86	2,24	1:45 ≈ 1:40
tnt8 (2)		955,5 ng/µl	19110	10297	1,86	2,23	
a Water		-0,2 ng/µl	-3	-3	1,22	0,41	
tnt9	14682	1427,2 ng/µl	28544	15683	1,82	2,21	1:70
tnt9 (2)		1509,2 ng/µl	30183	16606	1,82	2,21	
a Water		-1 ng/µl	-20	-16	1,22	0,61	
a Water		0,1 ng/µl	1	-2	-0,46	0,02	
tnt10	5327	530,5 ng/µl	10610	5737	1,85	2,17	1:25
tnt10 (2		534,9 ng/µl	10699	5807	1,84	2,18	
a Water		0,1 ng/µl	1	-2	-0,23	0,11	
tnt11	5639	578,5 ng/µl	11569	6498	1,78	1,96	1:27
tnt11 (2		549,3 ng/µl	10986	6186	1,78	1,99	
a Water		-0,2 ng/µl	-4	-9	0,47	0,57	
tnt8 2elucion	653	647,9 ng/µl	12958	6937	1,87	2,17	1:32
tnt8 2elucion (2)		658,1 ng/µl	13161	7099	1,85	2,17	
a Water		-0,6 ng/µl	-11	-20	0,56	0,45	
a Water		0,1 ng/µl	-1	-2	0,36	0,33	

Figure-7

2.2.2 Electrophoretic Analysis of DNA Quality

Electrophoresis is probably the most common means of examine molecular distribution of both simple and complex DNA samples and the easiest method for evaluating genomic DNA integrity.

All 23 isolated DNAs were electrophoretically arrayed onto a 0.8% Seakem LE (*LONZA*) agarose gel made with 1X TBE buffer (dilution 1:10 of 10X sterile, DNAases, RNAases and proteases free TBE made with 1M Tris, 0.9M Boric Acid and 0.01M EDTA). To achieve the most accurate dsDNA quantitations, gels were stained with ethidium bromide and SYBR-Green I (fluorescent dsDNA specific dye) diluted to final concentrations of 0.2 ug/ml and 1:10000 respectively. Three microliters of each DNA thouroughly mixed with 2ul of 6X Orange DNA gel loading dye (*Thermo Scientific*) were loaded in the gel. Electrophoresis was performed in a horizontal electrophoresis chamber *(Owl™ A5 Large Gel System with Built-In Recirculation, from Thermo Fisher Scientific)* at 85 Volts (*Voltage font: Owl™ EC-300XL, from Thermo Scientific*) for approximately 3 hours. To evaluate the size of fragmented DNA, a molecular weight marker of 100bp – 1Kb (*ExACTGene Fisher Bioreagents*) was loaded next to the samples.

Finished the electrophoresis the agarose gels were visualized in the Gel Doc™ XR System from *BioRad,* which includes filters for both ethidium bromide and SYBR- GREEN. **Figure 8** Illustrates the electrophoresis of the 8 samples (TNT8 to 11) previously quantified in the Nanodrop (see **Figure 7** above). The first 4 lanes correspond to samples TNT 8 to TNT 11, the fifth lane corresponds to the second elution of TNT8.

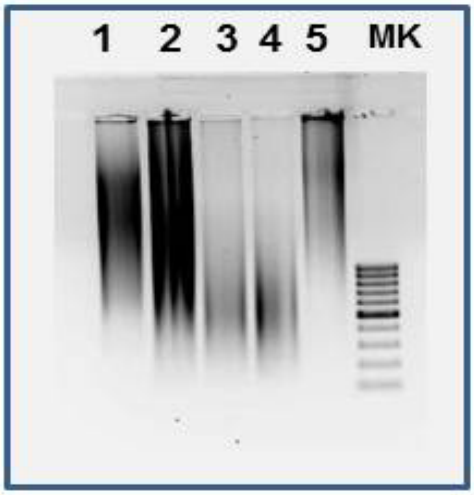

Figure 8

2.3 DNA amplification by Polymerase Chain Reaction

Polymerase chain reaction (PCR) is an established in vitro method of nucleic acid synthesis, widely used in molecular biology to exponentially amplify a region of genomic DNA in which we are interested. It involves two oligonucleotide primers (sense and antisense) that flank the DNA fragment to be amplified and repeated cycles of: 1) heat denaturation of target DNA; 2) primer annealing to complementary DNA sequences; and 3) extension of the annealed primers with thermostable DNA polymerase. Oligonucleotide primers hybridize to opposite strands of the target sequence and oriented so that DNA synthesis by the polymerase proceeds across the region between them. Since the extension products themselves are also complementary to and capable of binding primers, successive cycles of amplification essentially double the amount of target DNA synthesized in the previous cycle. The result, therefore, is an exponential accumulation of a specific fragment of DNA, approximately 2^n, where **n** is the number of cycles of amplification performed.

In a typical polymerase chain reaction genomic DNA is incubated a 3 temperatures corresponding to the 3 steps (denaturation, annealing and extension) of each cycle of amplification. Double-stranded DNA is commonly denatured by heating to 90-95ºC for approximately 30 seconds. When such denaturation is incomplete DNA strands snap back reducing the yield product. To avoid PCR failure due to incomplete denaturation of target DNA it is helpful to precede the first cycle of amplification with an initial denaturation step of 8-10 minutes at 95ºC. Once achieved enough strand separation, sense and antisense primers anneal to their complementary target sequences by briefly cooling to 40-60ºC. Stringent annealing temperatures (>55ºC) are known to increase target specificity and therefore fidelity in the final PCR product. Extension of the annealed primers with thermostable Taq DNA polymerase requires heating template to 70-75ºC. The time of incubation at 70-75ºC varies according to the length and concentration of target sequence being amplified. Optimization of cycle number is the best way to avoid amplifying background products. The number of cycles depends mainly upon the starting concentration and quality of target DNA. Amplification of DNA from paraffin-embedded tissues as in our case is less efficient than that from other templates such as frozen tissues, cell lines,…., thus, it is necessary to compensate increasing the number of cycles and lengthening the time at each temperature within the cycle. A final elongation step at 72ºC for 10 minutes brings the new DNA molecules, when replication finishes.

The PCR reaction is performed in 0.2 ml microtubes and involves the following reagents that besides the thermocycling features also influence the specificity, fidelity and yield of the desired product:

- *10X reaction Buffer free of MgCl2* [75mMTris HCl (pH9.0, 50mM KCl, 20mM (NH4)2SO4] (*Biotools*) diluted 1:10 in the final volume of PCR (30 ul in our case). The buffer regulates the pH of the PCR. The pH during the PCR reaction is important because affects the activity and fidelity of the Taq DNA polymerase.
- *Magnesium Chloride* concentration (MgCl2) (50mM Biotools). Results pivotal in the PCR reaction because affects the proper functioning of the Taq DNA polymerase. A concentration below that necessary may inactivate the enzyme and a concentration above the optimum may reduce the fidelity of the enzyme and favour unspecific annealings and, thus, unexpected products. In general MgCl2 ranges between 1.5 mM and 3.5mM
- *Primers / oligonucleotides concentration and composition (Sigma, Invitrogen, Thermo,* …..). In general primer concentrations range between 0.25 µM and 0.5 µM. Respect primer pair composition, most efficient oligonucleotides are 20 to 30 nucleotides in length with an average G+C content around 50-55%. It is also important to avoid palindromic sequences, complementarity at the 3` ends and secondary structures if possible.
- *Deoxynucleotide Triphosphates (dNTPs) concentration (Fermentas 100mM)*. The optimum concentration is about 0.2mM and all four (dATP, dGTP, dCTP and dTTP) must be balanced.
- *Taq DNA polymerase concentration (Biotools).* It is the enzyme that catalyzes the synthesis of new molecules of DNA. The optimum concentration is roughly 40mU/µl.
- H2O free of nuecleases, not DEPC treated (Invitrogen – Ambion) till complete the final volume of the PCR reaction that in our case as mentioned before is 30 µl.
- *Concentration and quality of input DNA*. Essentially any sample subjected to amplification should contain at least one intact DNA strand encompassing the region to be amplified and impurities must be sufficiently diluted so that they do not inhibit the reaction. The average concentration of DNA used in the PCR reaction ranges between 20 ng/µl and 100 ng/µl

In order to establish the optimum PCR conditions and achieve the maximum efficiency, specificity and fidelity in the amplification of genes of our interest, first of all it is important to perform a gradient temperature PCR. The latter technique allows us to establish not only the best annealing temperature but also the optimum concentration of MgCl2, dNTPs and primers.

In parallel to the amplification of the *TERT* promoter region, encompassing the “hot spot” mutation zones, in this study were amplified by means of PCR the following genomic regions:

- activation loop of *BRAF*
- GTP-binding domain and GTP-ase domain of the three *RAS* genes.

Optimum PCR conditions for all 8 genomic regions were previously established. **Table-1** shows the size of the resulting PCR product, the sense and antisense oligonucleotide sequence, the annealing temperature and the choice MgCl2 concentration. The dNTPs concentration was in all cases 0,2 mM

Table-1

Gen or exon to amplify	Primers sequence	Size (bp)	Annealing temperature	[Primers] uM	[MgCl2] mM
TERT promoter	[+]5'-TCCCTCTCAGGCATAAGGTAA-3'	145	60	0,5	2,5
	[-]5'-CGAACAGTGAATATTTCCTTTGAT-3'				
BRAF exon 15	[+]5'-TCATAATGCTTGCTCTGATAGGA-3'	226	60	0,25	1,5
	[-]5'-GGCCAAAAATTTAATCAGTGGA-3'				
K-RAS exon 1	[+]5'-GACTGAATATAAACTTGTGG-3'	163	55	0,5	2,5
	[-]5'-CTGTATCAAAGAATGGTCCT-3'				
H-RAS exon 1	[+]5'-CAGGCCCCTGAGGAGCGATG-3'	110	60	0,5	1,75
	[-]5'-TTCGTCCACAAAATGGTTCT-3'				
N-RAS exon 1	[+]5'-GACTGAGTACAAACTGGT-3'	118	58	0,25	2,5
	[-]5'-GGGCCTCACCTCTATGGT-3'				
N-RAS exon 2	[+]5'-GGTGAAACCTGTTTGTTGGA-3'	103	55	0,25	4
	[-]5'-ATACACAGAGGAAGCCTTCG-3'				

Two 0.2ml microtubes without template DNA, closed before and after adding the DNA to the remaining tubes, were enclosed as white/negative controls on each amplification reaction to check the purity of all reagents and handling DNA cross contamination respectively. PCR reactions were performed in two thermocyclers from *Applied Biosystems*, the *SimpliAmp Thermal Cycler and the Veriti Thermal Cycler*

PCR efficiency was verified by means of electrophoresis of yield products onto 3% agarose Seakem LE (LONZA) gels made with 1X TBE buffer and stained with ethidium bromide (Invitrogen) diluted to 0.2µg/ml. Electrophoresis was carried out at 125 Volts for 45 minutes in the *Owl™ A5 wide Gel horizontal Gel System with Built-In Recirculation, from Thermo Fisher Scientific.* The fluorescence generated by ethidium bromide /DNA complexes after 254 nm ultraviolet trans-illumination was captured in the Gel Doc™ XR System from *BioRad*. The length of PCR products separated by gel electrophoresis was estimated by comparison with a low range DNA ladder (25-700 bp – O`Gene ruler – Fisher Bioreagents). **Figure 9** displays some examples of the PCRs performed in the 8 genomic regions.

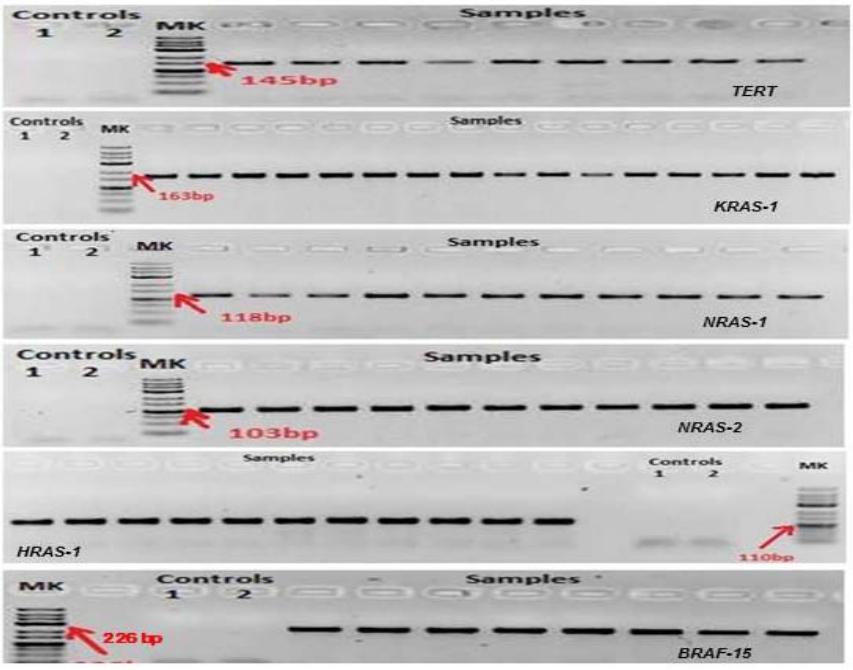

Figure 9

2.4 Analysis of mutations at *BRAF* and *K-, N-* and *H-RAS* by means of Single Strand Conformational Polymorphism (SSCP) technique

Single **S**trand **C**onformational **P**olymorphism (**SSCP**) is a technique based on the known principle that electrophoretic mobility of any particle within a gel is sensitive to both its size and shape. Under non-denaturing conditions a single-stranded (ssDNA) molecule has a folded conformation or secondary structure that is determined by its intramolecular interactions and, thus, by its sequence. Accordingly, ssDNA molecules differing by as little as a single nucleotide substitution in a several hundred base pair sequence may feature different secondary structures, which results in altered mobility in non-denaturing gel electrophoresis. To scan genomic DNA for mutations or SNPs, the PCR products from interrogated samples, which have been preferentially amplified on the same PCR, are subjected to denaturation or strand dissociation by heating in the presence of formamide. The double–stranded character of the amplified DNA fragments is eliminated and folded single-stranded secondary structures emerge during nucleic acid cooling. Such three dimensional structures are unique to the primary sequence of the nucleic acid and migrate at different rates through non-denaturing gels. Detection of unknown point mutations, therefore, relies on the differences seen in the electrophoretic mobility of separated single DNA strands from wild type and mutant target sequence. A mutated gene will show one or both strands shifted compared to the migration pattern of the wild type gene

Under optimum SSCP conditions is possible to detect as little as 0.1%-0.2% of mutant contribution to total target assayed. The overall rate of mutation detection varies with the size of the DNA molecule interrogated, decreasing in fragments larger than 300bp and shorter than 100bp. In addition to the size of the target DNA, sensitivity of SSCP for detection of single base substitutions may result affected by several factors such as the ionic strength of the running buffer, the nature of the gel matrix and the temperature of the gel during electrophoresis. Complementary single strands are better separated in gels with low crosslinking, which have an increased pore size, circumstances both that make non-denaturing gels more sensitive to changes in DNA conformation. It`s also important to avoid ohmic heating and to keep and efficient cooling throughout the gel during electrophoresis. A temperature rise during gel running may destroy some semi-stable single-stranded DNA conformations hampering to detect single nucleotide substitutions and to obtain reproducible results. For higher SSCP resolution special gel matrices such as MDE (**M**utation **D**etection **E**nhancement Gel matrix) are also commercially available (LONZA). Optimization of SSCP conditions, therefore, depends on the characteristics of the DNA fragment to be screened and must be established empirically.

For SSCP analysis of *BRAF* and *RAS* genes, 30-40ng of PCR product were denatured by adding 2.5 to 5 volumes of Stop Solution (100% formamide, 5.0 M NaOH, 1% bromophenol blue and 1% xylene cyanol) and heating at 95ºC for 5 min. After quick chill on ice, samples were loaded onto 40% MDE gel matrices (2X MDE stock solution diluted in deionized water and 5X TBE to 0.8X working solution) for all exons genotyped (*BRAF exon 15, NRAS exon 1 and 2, KRAS exon 1 and 2 and HRAS exon 2*) but *HRAS* exon 1, which showed a better strand migration with 50% MDE gel matrices (2X MDE stock solution diluted in deionized water and 5X TBE to 1X working solution). Gel forming solution was mixed with 10% ammonium persulfate (10%APS) and TEMED for polymerazation. Standard 18 x16 cm long and 0.75 mm thick format gels were run in a vertical electrophoresis system (SE 600 Ruby Standard Dual Cooled Vertical Unit form GE Healthcare) filled with chilled (4ºC) 0.5X TBE and connected to a refrigerated circulating bath (Optima LTC2 form Grant) to keep an efficient cooling throughout the gel during the electrophoresis. **Table 2** shows the optimum SSCP conditions for detection of mutations at

the activation loop of *BRAF* (exon 15) and the GTP-binding and GTP-ase domains of the three *RAS* genes (exons 1 and 2).

Gen and exon	MDE concentration	Voltage (V)	Temperature (ºC)	Time (hours)
BRAF exon 15	0,8X	180	10	10:30-11
K-RAS exon 1	0,8X	400	18	4
K-RAS exon 2	0.8x	180	10	11-12
H-RAS exon 1	1X	300	18	6:45
H-RAS exon 2	0,8x	400	18	5
N-RAS exon 1	0,8X	300	18	6
N-RAS exon 2	0,8X	400	18	4:30

Table 2

After electrophoresis SSCP gels were stained in a shaker, in the dark, with SYBR Gold nucleic acid gel stain (Invitrogen) diluted 1:10000 in 1X TBE buffer, during 5-30 min. Before proceeding with gel imaging in the Gel Doc™ XR System the MDE gels were washed with running tap water to remove excess of SYBR Gold.

All samples were run in duplicate to assess the reproducibility of the migration pattern in two independent PCR products of the DNA sample assayed. Reproducible mobility shifts were cut and re-suspended in TE buffer. A microliter of the DNA eluted in the TE buffer was taken afterwards to be amplified using the same PCR conditions used with the original DNA but less number of cycles (n=35). The resulting PCR products were purified for subsequent sequencing using the commercial column based kit "GFX™ PCR DNA and Gel Band Purification Kit", from *illustra GE HealthCare* (see procedure below - point 2.5)

Figure 10A shows the characteristic wild type *BRAF* exon 15 (activation lop) SSCP pattern and the typical mobility shift found when the mutant V600E is present at *BRAF* exon 15. **Figure10B** shows the characteristic wild type *NRAS* exon 2 (GTPase domain) SSCP pattern and the typical mobility shift seen when the mutant Q61R is present in *NRAS* exon 2. **Figure 10C** shows the characteristic wild type *KRAS* exon 1 (GTP binding domain) SSCP pattern and the characteristic mobility shifts observed when the mutant G12D is present in *KRAS* exon 1.

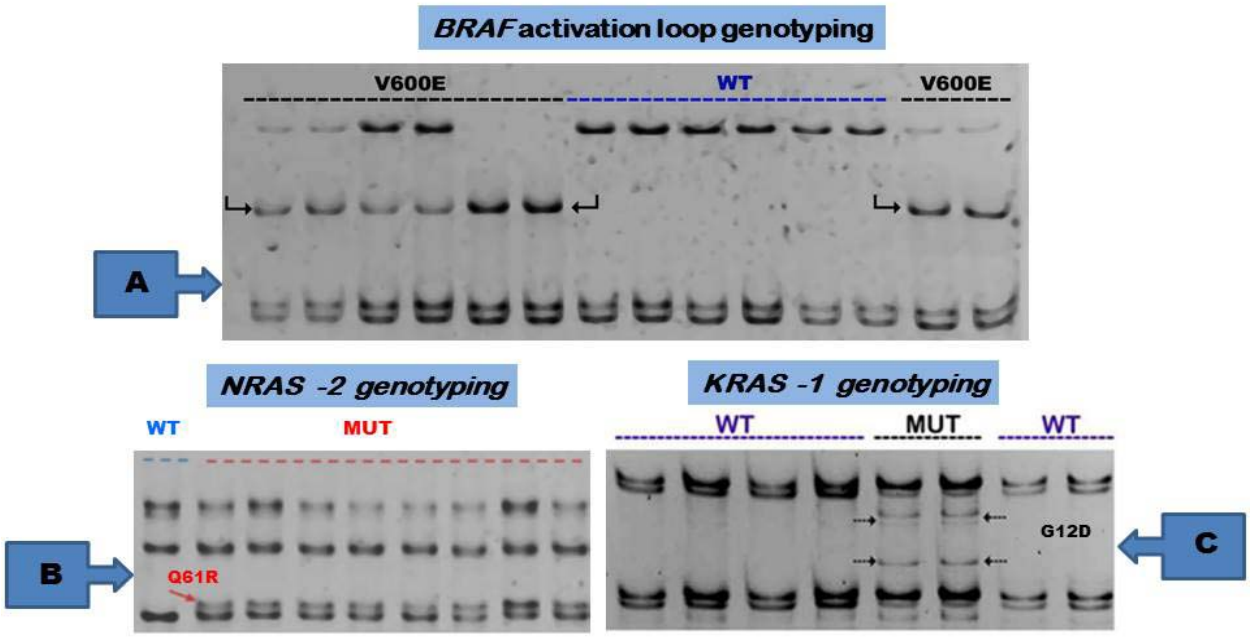

Figure 10

2.5 Analysis of mutations at *TERT* promoter region by means of PCR amplification and Direct Sequencing

The *TERT* promoter PCR products were purified for subsequent sequencing using the commercial kit GFX™ PCR DNA and Gel Band Purification Kit, by *illustra GE HealthCare.* This is a column based kit designed for practicing rapid purifications of PCR products or DNA fragments ranging in size between 50bp and 10kb. It Removes 99,5% of the contaminants.

Purification can be approached in two ways depending on the presence or not of unspecific bands in the PCR product to be purified:

I. When unspecific bands are present, the PCR product is mixed with 1.5 µl of 6X Orange loading dye (*Thermo Scientific*) and loaded onto a 2% SEAKEM LE agarose gel (*LONZA*) made with 1X TBE and stained with ethidium bromide (*Invitrogen*). Once the unspecific bands are sufficiently separated from the band containing the DNA we are interested to purify, the latter band is cut and dissolved in 300µl of capture buffer provided with the kit. To facilitate the disintegration of the agarose, which may seriously interfere with capillary sequencing, the tubes containing the excised bands re-suspended in capture buffer are vigorously vortexed and mixed by inversion while heated 30 minutes at 60ºC in a Heating block (Grant QBD2). Completed the melting of agarose the capture buffer containing the amplified target DNA free of unspecific contaminants is transferred to the purification column provided with the kit assembled to a collection tube.

II. When the PCR products to be purified do not have unspecific bands the electrophoresis in agarose gels is skipped and the PCR products are mixed directly with 300µl of capture buffer in the purification column assembled to a collection tube.

The capture buffer is composed basically of isopropanol and it works attaching the DNA to the membrane present in the columns. The following steps of the purification process are equal for PCR products with and without unspecific bands. Briefly:

- Incubation 1 min at room temperature
- Centrifugation at maximum speed (13000 rpm) 1 minute to facilitate DNA binding to the membrane
- Discard of volume retrieved in the collection tube
- Washing the purification column with 500µl of washing buffer (basically ethanol) provided with the kit. The objective is to eliminate all the PCR reagents that are not bound to the membrane (primers not consumed, dNTPs, salts,…..)
- Centrifugation at maximum speed (13000 rpm) for 2 minutes
- Discard of volume retrieved in the collection tube
- Centrifugation of the empty purification column at maximum speed (13000 rpm) for 30 seconds
- Discard of volume retrieved in the collection tube
- Transfer of the purification column to a storing tube and elution of DNA attached to the membrane. The elution buffer provided with the kit consists of dH2O. The elution volume will depend of the strength / potency of the PCR product purified (average 15ul to 45ul)
- Incubation at room temperature 1 minute

- Centrifugation at maximum speed (13000 rpm) 1 minute
- Discard of purification column

The efficiency of the purification is checked by means of electrophoresis on 2% agarose SEAKEM LE gels (LONZA) of purified products mixed with loading dye buffer (bromophenol blue or xylene cyanol depending on the size of the purified product). After 30- 40min of electrophoresis, we can visualize the purified products in the Gel Doc System, as commonly.

The efficiency will be determinant in the decision of sending to sequencing or not the purified product. The sequencing reaction and the subsequent sequencing in a sequencer analyser (ABI PRISM 3700 – Perkin Elmer) will not work properly if the purified product that we see in the agarose gel is weak. **Figure 11** illustrates the purification of *TERT* products by means of excised agarose gel bands containing the target DNA. **Figure 11A** corresponds to the step in which all the PCR volume is loaded in the gel. Based on the potency of the bands, in this particular case, for the brightest bands we decided to use a final elution volume of 18 µL and for the weaker ones a volume of 13µL. **Figure 11B** shows the efficiency of the purified products. As we can see, some of the elution volumes chosen were not exactly right, because the concentration of some DNAs is too low to function properly in Sanger Sequencing.

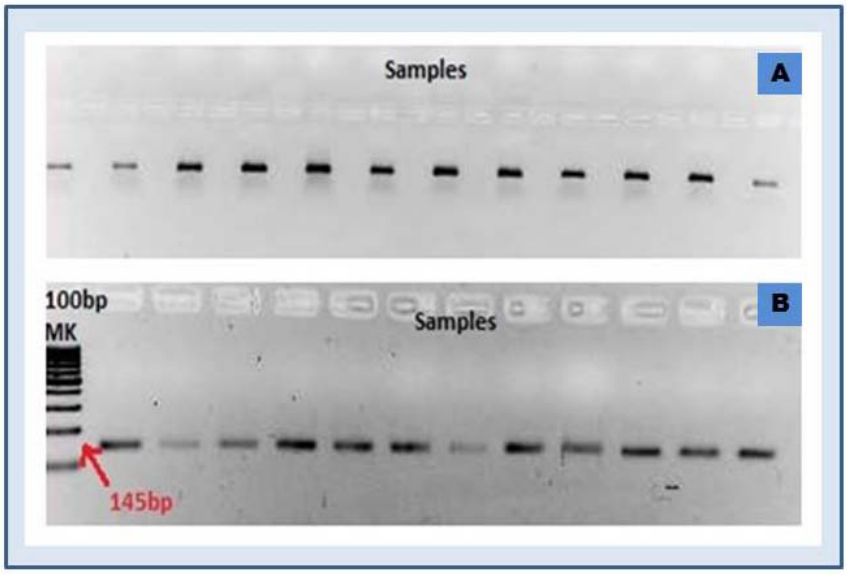

Figure 11

Results

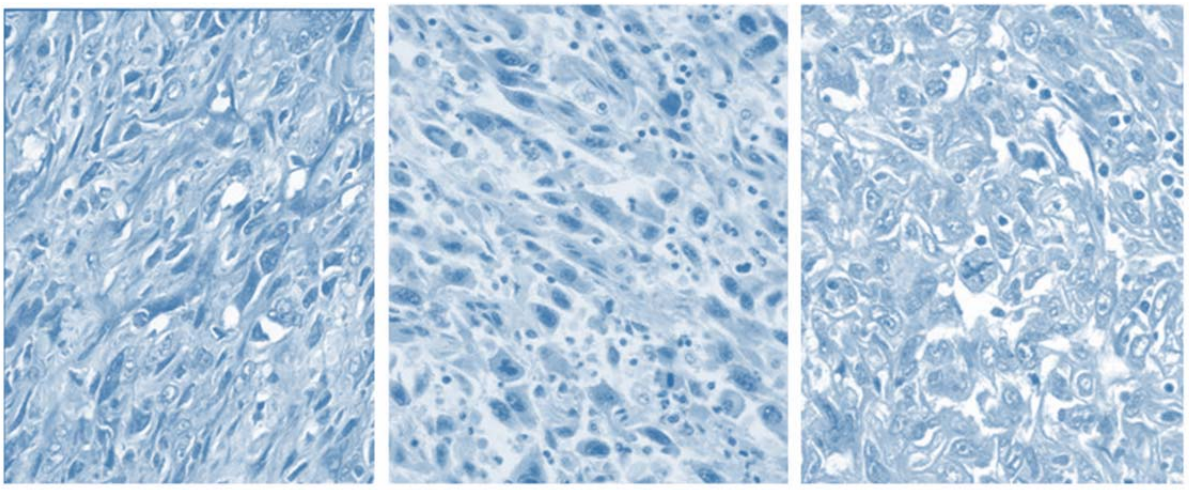

1. Analysis of mutations in the *TERT* promoter region in ATCs

Genotyping of ***TERT*** promoter region revealed a mutation prevalence of 67% (6 out of 9 cases). All of the mutations seen were transitions, involving the substitution of a Cytosine by a Tyrosine in the nucleotide sequence. No other type of mutation besides the substitution of a Cytosine by a Tyrosine either 124 base pairs or 146 base pairs upstream the transcription start site was seen in this study

- **C228T** (c.1-124 C>T) displayed by five cases (56%)
- **C250T** (c.1-146 C>T) displayed by one case (11%)

TUMOR HISTOTYPE	*TERT* promoter mutational analysis			TOTAL
	Mutated cases		WT cases	
	c.1-124 C>T	c.1-146 C>T		
Anaplastic Thyroid Carcinomas (ATCs, n = 9; Areas genotyped = 23)	5 (56%)	1 (11%)	3 (33%)	9

The following Figure shows three different **ATC** cases [283, 281 and 287] mutated either 124 base pairs upstream (**C228T**) or 146 base pair upstream (**C250T**) the transcription start site of the ***TERT*** gene. Mutations do not seem to associate with specific subtypes of **ATC** [sarcomatoid, epithelioid, squamous, small cells]

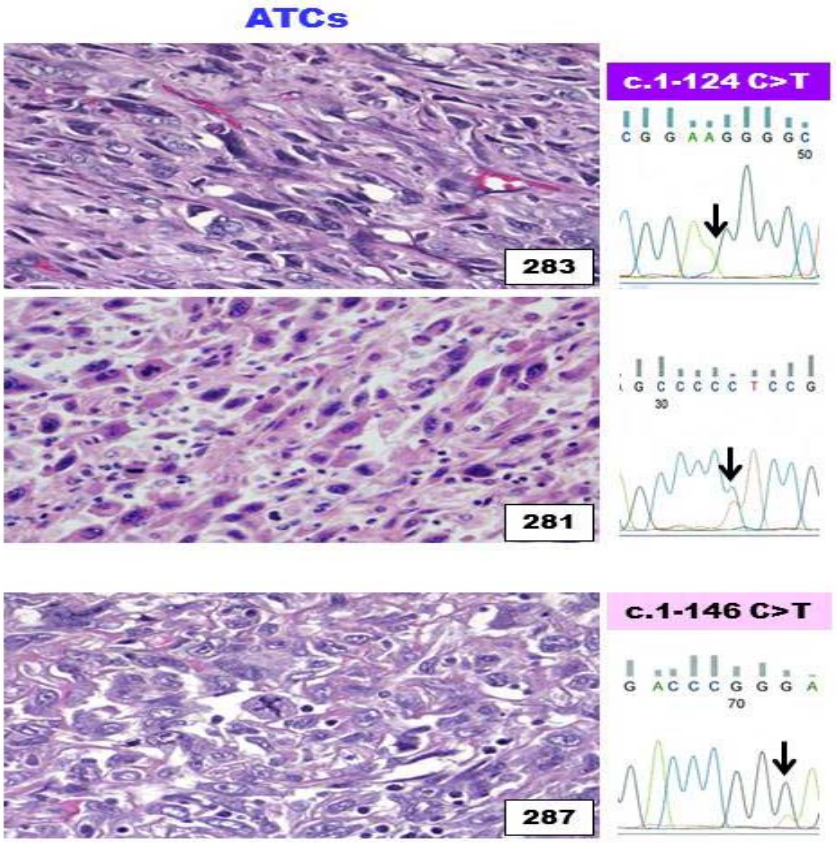

Focusing on mutated cases, the following figure illustrates the mutation distribution among the six mutated cases.

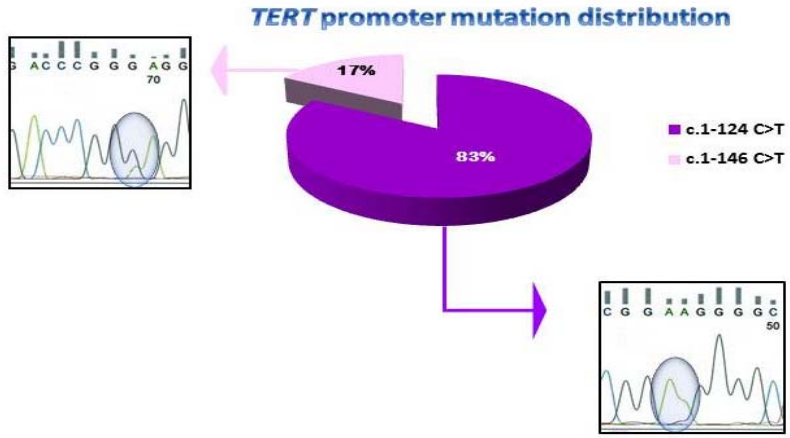

The mutation **C228T** (c.1-124 c>T) is far more common than the **C250T** (c.1-146 C>T), representing 83% of the mutations detected in this series.

2. Clonal or Subclonal character of *TERT* promoter mutations

The analysis of areas of concurrent better-differentiated thyroid carcinoma foci, areas with different microscopic appearance (e.g. spindle / sarcomatoid like or giant cell / epitheliod pattern of growth within the same **ATC**) but the same histological grade within the same biopsy revealed that ***TERT*** promoter mutations (**C228T** and **C250T**) are clonal in all of the cases genotyped.

The following figure illustrates the clonal nature of the c.1-124 C>T (**C228T**) mutation in two **ATC** cases exhibiting a concurrent better differentiated component within the same biopsy, more specifically an area of poorly differentiated thyroid carcinoma (**PDC**).

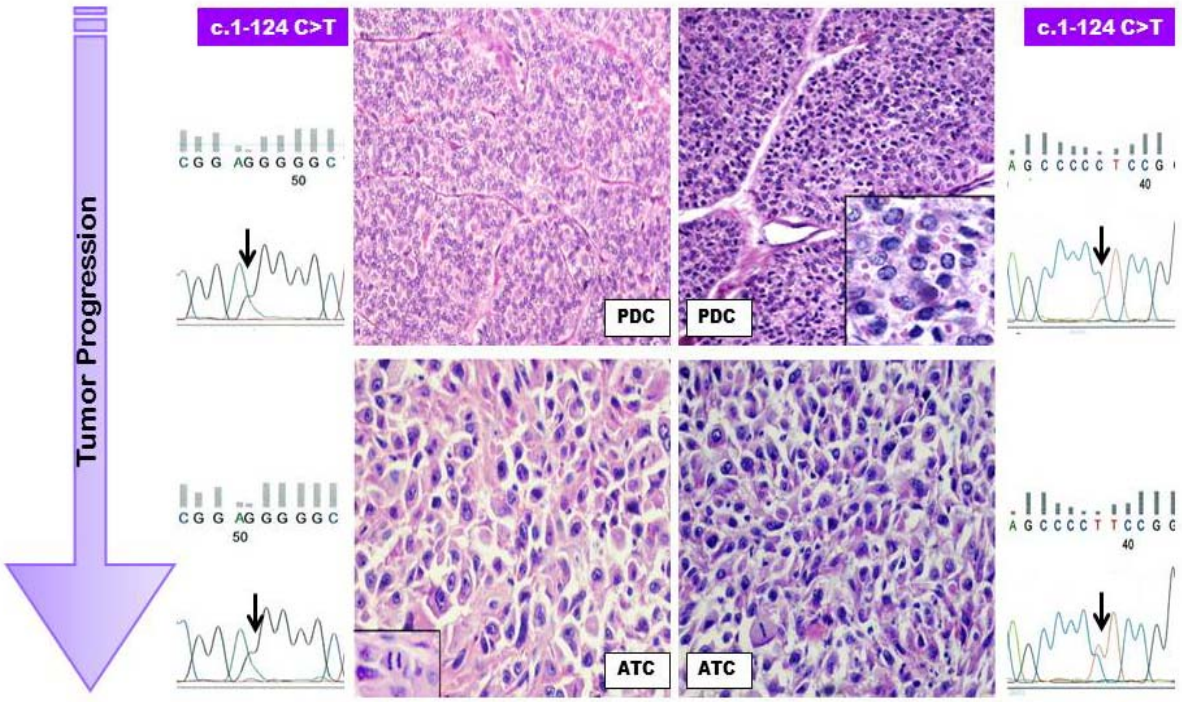

3. Segregation of *TERT* promoter mutations with tumor progression – de-differentiation or metastatic cells

In all of the cases in in which a concurrent better differentiated component, either a papillary thyroid carcinoma (**PTC**) area or a poorly differentiated thyroid carcinoma (**PDC**) area, were genotyped the mutation segregated with tumor progression differentiation.

ID		Histology	*TERT* c.1-124C>T	*TERT* c.1-146 C>T	*TERT* promoter
281	281A	ATC	c.1-124 C>T	WT	Y
	281B	PDC	c.1-124 C>T	WT	Y
283	283A	ATC	c.1-124 C>T	WT	Y
	283B	PDC	c.1-124 C>T	WT	Y
284	284A	ATC	c.1-124 C>T	WT	Y
	284B	PDC progressing	c.1-124 C>T	WT	Y
	284C	PTC	c.1-124 C>T	WT	Y
285	285A	ATC	c.1-124 C>T	WT	Y
	285B	PDC invading mediastinal muscle	c.1-124 C>T	WT	Y
	285C	PTC mixed oncocitoid	c.1-124 C>T	WT	Y
	285D	LNM of ATC	c.1-124 C>T	WT	Y
287	287A	ATC	WT	c.1-146 C>T	Y
	287B	PDC	WT	c.1-146 C>T	Y
	287C	ATC	WT	c.1-146 C>T	Y
	287D	LNM of PDC progressing	WT	c.1-146 C>T	Y
	287E	PDC progressing	WT	c.1-146 C>T	Y

The following figure shows the segregation of the c.1-124 C>T (**C228T**) mutation with tumor de-differentiation, progression in an epithelioid **ATC** case with a concurrent Poorly Differentiated Thyroid carcinoma area (**PDC**) within the same biopsy.

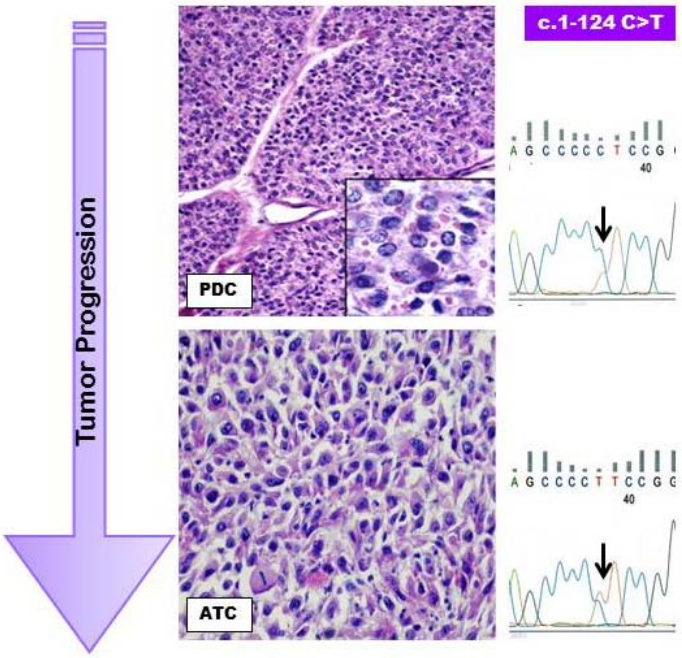

Regarding the segregation of ***TERT*** promoter mutations with metastatic cells, the table above shows that the two cases in which this situation was feasible to evaluate (285 and 287), in both cases the mutations (**C228T** → case 285 and **C250T** → case 287) segregated with cells invading surrounding tissues, lymph node or distant sites.

4. Coexistence of *TERT* promoter mutations with other common oncogenic events in ATCs

In order to establish if ***TERT*** promoter mutations associate with mutations at ***BRAF*** or ***RAS***, as it has been postulated by some authors and at the same time put some light in this controversial issue, mutations at the activation loop of ***BRAF*** and the GTP-binding domain and GTP-ase domain of the three ***RAS*** genes were characterized in the 9 cases included in this study. Genotyping was done by means of Single Stranded Conformational Polymorphism (SSCP) and direct sequencing

The following table shows the results of such analysis.

ID		Histology	BRAF-15	BRAF	K-RAS-1	N-RAS-1	N-RAS-2	H-RAS-1	RAS	TERT c.1-124C>T	TERT c.1-146 C>T	TERT promoter
280	280A	ATC	Q612Stop	Y	WT	WT	WT	WT	N	WT	WT	N
	280B	ATC	Q612Stop	Y	WT	WT	WT	WT	N	WT	WT	N
281	281A	ATC	Q612Stop	Y	WT	WT	Q61R	WT	Y	c.1-124 C>T	WT	Y
	281B	PDC	Q612Stop	Y	WT	WT	Q61R	WT	Y	c.1-124 C>T	WT	Y
282	282A	ATC	WT	N	G12D	WT	WT	WT	Y	WT	WT	N
	282B	PDC	WT	N	G12D	WT	WT	WT	Y	WT	WT	N
	282C	Clear cells progressing	WT	N	G12D	WT	WT	WT	Y	WT	WT	N
283	283A	ATC	WT	N	WT	WT	Q61R	WT	Y	c.1-124 C>T	WT	Y
	283B	PDC	WT	N	WT	WT	Q61R	WT	Y	c.1-124 C>T	WT	Y
284	284A	ATC	V600E	Y	WT	WT	WT	WT	N	c.1-124 C>T	WT	Y
	284B	PDC progressing	V600E	Y	WT	WT	WT	WT	N	c.1-124 C>T	WT	Y
	284C	PTC	V600E	Y	WT	WT	WT	WT	N	c.1-124 C>T	WT	Y
285	285A	ATC	WT	N	WT	WT	Q61R	WT	Y	c.1-124 C>T	WT	Y
	285B	PDC invading mediastinal muscle	WT	N	WT	WT	Q61R	WT	Y	c.1-124 C>T	WT	Y
	285C	PTC mixed oncocitoid	WT	N	WT	WT	Q61R	WT	Y	c.1-124 C>T	WT	Y
	285D	LNM of ATC	WT	N	WT	WT	Q61R	WT	Y	c.1-124 C>T	WT	Y
286	286	ATC	V600E	Y	WT	WT	WT	WT	N	c.1-124 C>T	WT	Y
287	287A	ATC	WT	N	WT	WT	WT	WT	N	WT	c.1-146 C>T	Y
	287B	PDC	WT	N	WT	WT	WT	WT	N	WT	c.1-146 C>T	Y
	287C	ATC	WT	N	WT	WT	WT	WT	N	WT	c.1-146 C>T	Y
	287D	LNM of PDC progressing	WT	N	WT	WT	WT	WT	N	WT	c.1-146 C>T	Y
	287E	PDC progressing	WT	N	WT	WT	WT	WT	N	WT	c.1-146 C>T	Y
288	288	ATC	WT	N	WT	WT	WT	WT	N	WT	WT	N

The overall prevalence of ***BRAF*** mutations was 45% (4 out of 9 cases). Two types of mutations were found. The prevailing **V600E** (c.1799C>A) and the truncating **Q612*** (c.1834C>T). Both reported in COSMIC

TUMOR HISTOTYPE	*BRAF* mutational analysis			TOTAL
	Mutated cases		WT cases	
	V600E	Other [Q612Stop]		
Anaplastic Thyroid Carcinomas (ATCs, n = 9; Areas genotyped = 23)	2 (22%)	2 (22%)	5 (55%)	9

Focusing on mutated cases, the following figure illustrates the mutation distribution among the four mutated cases.

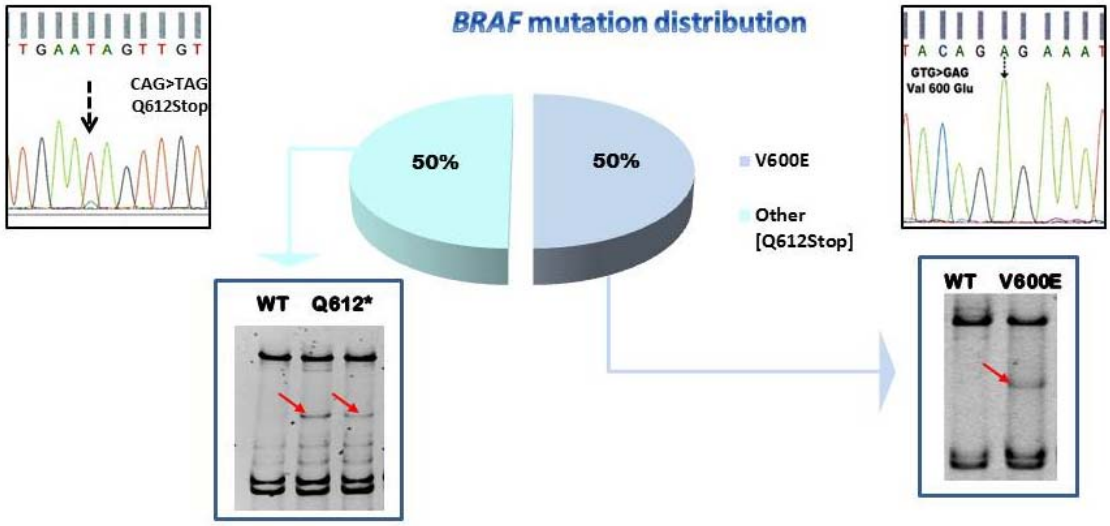

The overall prevalence of ***RAS*** mutations was 45% (4 out of 9 cases). Neither the GTP-binding domain of ***HRAS*** nor the GTP-binding domain of ***NRAS*** revealed a single mutation. Mutations were mainly at the GTP-ase domain of ***NRAS*** and less frequently at the GTP-binding domain of ***KRAS***.

TUMOR HISTOTYPE	*RAS* mutational analysis				TOTAL
	Mutated cases			WT cases	
	KRAS	NRAS	HRAS		
Anaplastic Thyroid Carcinomas (ATCs, n = 9; Areas genotyped = 23)	1 (11%)	3 (33%)	0	5 (55%)	9

Focusing on mutated cases, the following figure illustrates the mutation distribution among the four mutated cases.

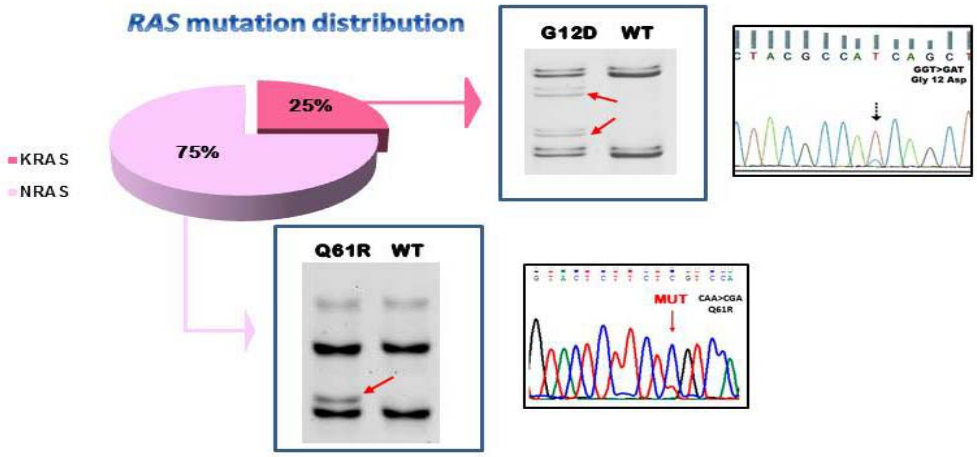

Similarly to what seen in ***TERT*** promoter screening, both ***BRAF*** and ***RAS*** mutations were clonal and segregated with tumor progression, de-differentiation and invading cells. See table above with all the mutations found in this study.

Regarding the coexistence of ***TERT*** promoter mutations with ***BRAF*** and/ or ***RAS*** mutations the study revealed that ***TERT*** promoter mutations coexisted with ***RAS*** or ***BRAF*** mutations in half of the cases screened respectively. One case (281) was concurrently mutated in ***BRAF***, ***RAS*** and ***TERT*** promoter.

The following figure shows the association of ***TERT*** promoter mutations at **C228T** and **C250T** with oncogenic events within the **MAPK** pathway

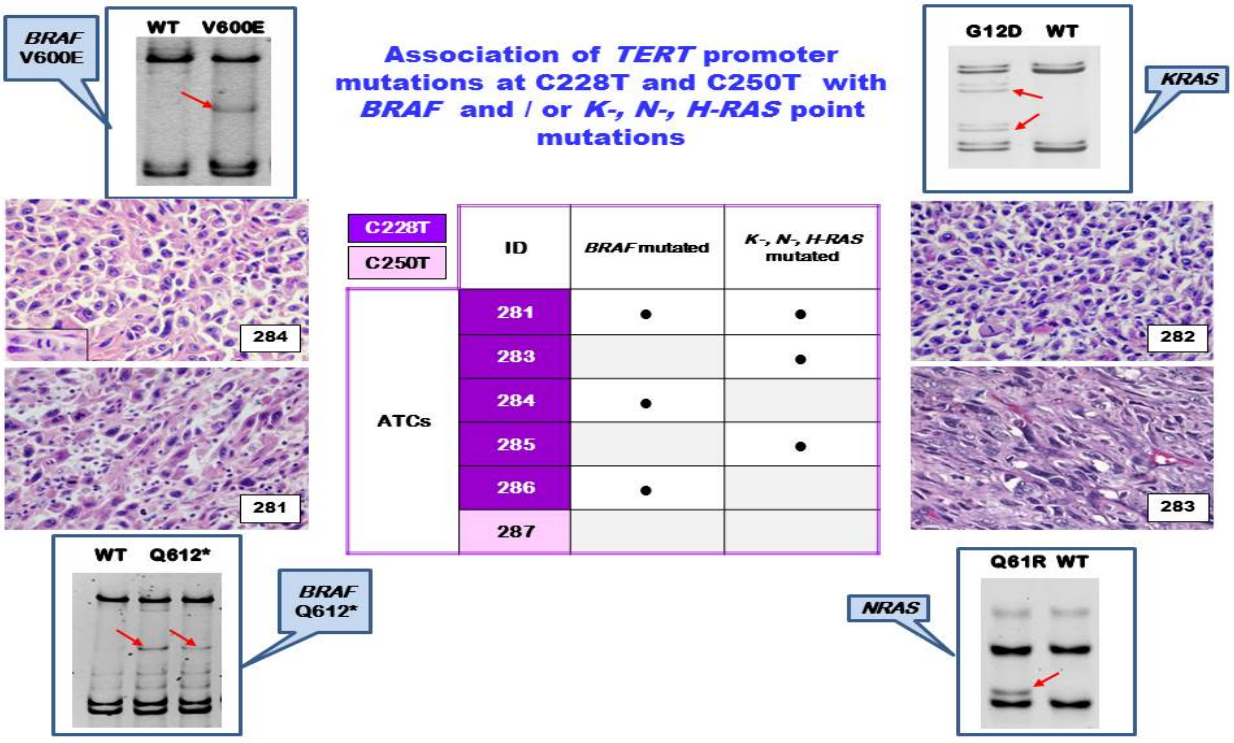

Concurrent activation of the **MAPK** pathway and the ***TERT*** promoter was seen in 83% of the mutated cases (5/6)

Discussion

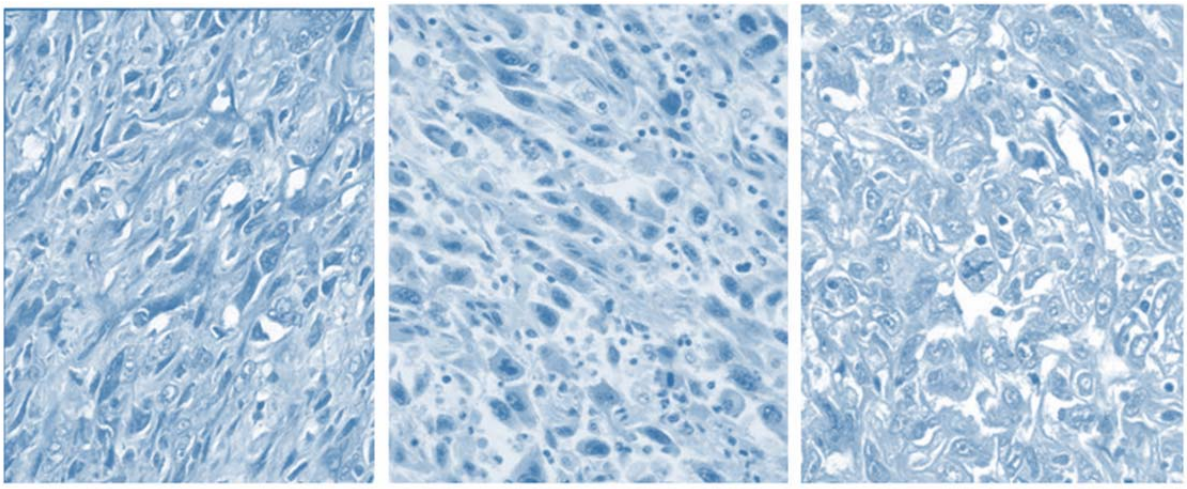

1. Analysis of TERT promoter mutations in ATC

The overall prevalence of ***TERT*** promoter mutations found in this study (67%) is in agreement with that reported so far in the literature (50%-73%). [16-19] Landa et al. found, in a recent study published in *Jounal of Clinical Investigation,* that ***TERT*** promoter mutations were one of the most prevalent oncogenic events among **ATCs**. ***TERT*** promoter mutations were equally prevalent to ***TP53*** mutations, being present both in 73% of the cases analysed (55 cases). [19]

Consistent with previous studies the mutation **C228T** (c.1-124 c>T) represents most of the mutations observed in the ***TERT*** promoter region (83%). Like in previous studies on **ATCs** the mutations **C228T** and **C250T** were mutually exclusive.[16-19]

2. Clonal or Subclonal character of *TERT* promoter mutations

To the best of our knowledge this is the first study that takes into consideration the clonality or subclonality of ***TERT*** promoter mutations.

In all of the ATC cases in which concurrent better differentiated thyroid carcinoma foci or areas with different microscopic appearance (e.g. spindle / sarcomatoid like or giant cell / epitheliod pattern of growth within the same ATC) but the same histological grade were genotyped (5/9 – 78% - all cases except 286 and 288), ***TERT*** promoted mutations emerged as a clonal event. Though the series of cases characterized in this study is small, it is unquestionably that shows a tendency. Furthermore, data in progress in the laboratory indicate that among **ATCs** ***TERT*** promoter mutations are unequivocally clonal. This is important because as probably some of you remember, when Noa Feas presented here her preliminary thesis data in advanced, metastatic, radioiodine resistant papillary thyroid carcinomas treated with Sorafenib, she showed that in some cases ***TERT*** promoter mutations are subclonal.

3. Segregation of *TERT* promoter mutations with tumor progression – de-differentiation or metastatic cells

The assessment of ***TERT*** promoter mutations role in tumor progression, dedifferentiation by means of genotyping concurrent better differentiated thyroid carcinoma areas present within the same biopsy represents also a new methodological approach. So far no one has analyzed the existence of ***TERT*** promoter mutations within concurrent better differentiated areas present in the same biopsy specimen. The data available correlating ***TERT*** promoter mutations with tumor dedifferentiation and progression have been inferred from ***TERT*** promoter mutation frequencies in Papillary Thyroid Carcinomas (PTC), Follicular Thyroid Carcinomas (FTC), Poorly Differentiated Thyroid Carcinomas (PDCs) and Anaplastic Thyroid Carcinomas (ATCs)

The same applies for the role of ***TERT*** promoter mutations in lymph node metastasis or distant metastasis. Only one recent study has characterized the prevalence of ***TERT*** promoter mutations in the primary tumor (Papillary Thyroid Carcinomas - PTCs) and matched lymph node or distant metastases. [20] Among **ATCs** no one has genotyped so far matched primary tumors and local or distant metastases. Though the number of cases in which I have characterized the primary tumor and paired lymph node or distant metastases is extremely low (2 cases→ 285 and 287), the results appear to indicate that ***TERT*** promoter mutations might play a role in metastases, particularly in distant metastases. The results are in agreement with data in progress in the lab and the TFM presented here in 2016 by Miriam Corraliza.

4. Coexistence of *TERT* promoter mutations with other common oncogenic events in ATCs

The overall prevalence of ***BRAF*** and ***RAS*** mutations found in this series is consistent with that reported in previous studies of **ATCs.** [19,21,22]

RAS mutation distribution is also consistent with previous reports. [19,21,22] Likewise ***RAS*** mutations locate preferentially at the GTPase domain of ***NRAS*** and the GTPbinding domain of ***KRAS***. [19,21,22]

In contrast with ***RAS*** mutations, ***BRAF*** mutation distribution is probably biased by the size of the cohort analyzed. The **V600E** (c.1799C>A) mutation, which is the commonest ***BRAF*** mutation in different tumor types including thyroid cancer in this series only represents half of the mutated cases (50%). In any case, the truncating Q612* mutation also deserves some attention. It has been found in a different series of primary papillary thyroid carcinomas and paired distant metastases that its being characterized in the laboratory. Though it would be necessary to characterize more tumors, the available results appear suggest that the Q612* mutation might play a role in tumor aggressiveness and metastases.

Similarly to ***TERT*** promoter mutations, ***RAS*** and ***BRAF*** mutations were clonal events. The clonality of ***TERT***, ***BRAF*** and ***RAS*** mutations suggest that are disease–driver mutations relevant in **ATC** behavior. It may relate with the rapidly progressive course of anaplastic thyroid tumors, conferring growth and aggressiveness advantages to the cells clones bearing one or more of such mutations.

In agreement with previous studies several of the tumors genotyped in this study were concurrently mutated in the ***TERT*** promoter region and ***BRAF*** or ***NRAS*** (83%). Nonetheless, in contrast with previous studies ***TERT*** mutations were not significantly correlated with ***BRAF*** or ***RAS*** mutations. This result may be influenced by the small size of the cohort analyzed. In any case the associations reported so far result controversial. For some groups ***TERT*** promoter mutations are significantly correlated with ***BRAF*** mutations, while for other groups the association is with ***RAS*** mutations [23].

Conclusions

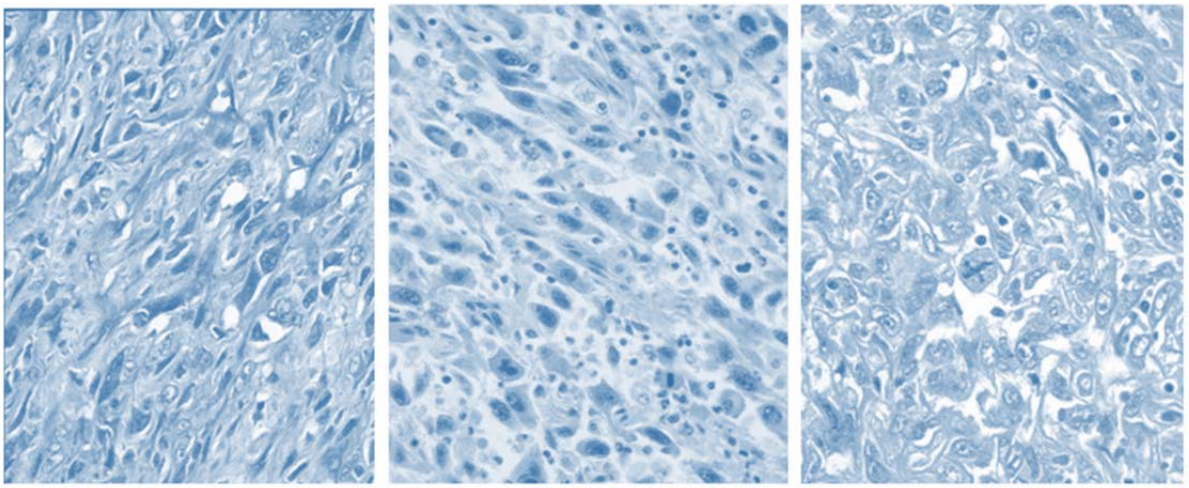

CONCLUSIONS:

- ***TERT* promoter mutations (C228T and C250T) are extremely frequent among ATCs (67%).**
- ***TERT* promoter mutations C228T and C250T are mutually exclusive.**
- **The C228>T promoter mutation is far more prevalent than the C250T mutation.**
- ***TERT* promoter mutations C228T and C250T appear to be clonal events, being present in the different areas genotyped within several tumors.**
- ***TERT* promoter mutations segregate with tumor dedifferentiation, being present in concurrent better differentiated areas analysed within several ATCs.**
- **Concurrent oncogenic activation of the MAPK pathway (e.g.** mutations in ***BRAF***, or ***RAS*) and *TERT* promoter is frequently seen among ATCs (83%)**

REFERENCES:

1. Hanahan, D. & Weinberg, R. *"Hallmarks of cancer: the next generation"* Cell 144(5), 646-74. (2011)
2. Jones, CL. & Kane, MA. *"Oncogenic signaling"* Current opinion in oncology 8(1), 54-9. (1996)
3. Mohebati, A. & Shaha AR. *"Anatomy of thyroid and parathyroid glands and neurovascular relations"* Clinical Anatomy 25(1), 19-31. (2012)
4. Carling, T. & Udelsman, R. *"Thyroid cancer"* Annual review of medicine 65, 125-37. (2014)
5. Thomas, G. *"Radiation and thyroid cancer: an overview."* Radiation Protection Dosimetry, ncy146. (2018)
6. Katoh*, H., Yamashita, K., Enomoto, T. & Watanabe, M. *"Classification and General Considerations of Thyroid Cancer"*. SciMedCentral. Review (2015)
7. WJ, S. *"Anaplastic thyroid carcinoma: a new approach."* Europe PMC 23(1), 25-27. (1980)
8. Giuffrida, D. & Gharib, H. *"Anaplastic thyroid carcinoma: Current diagnosis and treatmet."* SciMedCentral 11, 1083-1089. (2000)
9. M. Keutgen, X., M. Sadowski, S. & Kebebew, E. *"Management of anaplastic thyroid cancer"* Gland Surgery 4(1), 44–51. (2015)
10. Haddad, RI., Lydiatt, WM., Ball, DW., Busaidy, NL., Byrd, D, Callender, G., Dickson, P., Duh, QY, Ehya, H., Haymart, M., Hoh, C., Hunt, JP., Iagaru, A., Kandeel, F., Kopp, P., Lamonica, DM., McCaffrey, JC., Moley, JF., Parks, L., Raeburn, CD., Ridge, JA., Ringel, MD., Scheri, RP., Shah, JP., Smallridge, RC., Sturgeon, C., Wang, TN., Wirth, LJ., Hoffmann, KG & Hughes, M. *"Anaplastic Thyroid Carcinoma, Version 2"* JNCCN 13(9), 1140-50. (2015)
11. Leao, R., Dias Apolonio, J., Lee, D., Figueiredo, A., Tabori, U. & Castelo-Brando, P. "*Mechanisms of human telomerase reverse transcriptase (h*TERT*) regulation: clinical impacts in cancer"* Journal of Biomedical Science, 25:22. (2018)
12. Oishi N, Kondo T, Ebina A, Sato Y, Akaishi J, Hino R, Yamamoto N, Mochizuki K, Nakazawa T, Yokomichi H, Ito K, Ishikawa Y, Katoh R. *"Molecular alterations of coexisting thyroid papillary carcinoma and anaplastic carcinoma: identification of TERT mutation as an independent risk factor for transformation"* Nature (Modern Pathology) 30, 1527-1537. (2017)
13. Liu, R. Xing, M. *"TERT Promoter Mutations in Thyroid Cancer"* Endocr Relat Cancer 23(3), R143–R155. (2016)
14. Shi X, Liu R., Qu S., Zhu G., Bishop J., Liu X., Sun H., Shan Z., Wang E., Luo Y., Yang X., Zhao J., Du J., El-Naggar AK., Teng W. & Xing M. *"Association of TERT promoter mutation 1,295,228 C>T with BRAF V600E mutation, older patient age, and distant metastasis in anaplastic thyroid cancer"* The journal of clinical endocrinology and metabolism 100(4), E632-7. (2015)
15. Shi X, Liu R., Qu S., Zhu G., Bishop J,. Liu X., Sun H., Shan Z., Wang E., Luo Y., Yang X., Zhao J., Du J., El-Naggar AK., Teng W. & Xing M. *"Highly prevalent TERT promoter mutations in aggressive thyroid cancers"* Endocrine-related cancer 20(4), 630-10. (2013)
16. Romei C., Tacito A., Molinaro E., Piaggi P, Cappagli V., Pieruzzi L., Matrone A., Viola D., Agate L., Torregrossa L., Ugolini C., Basolo F., De Napoli L., Curcio M., Ciampi R., Materazzi G., Vitti P. & Elisei R. *"Clinical, pathological and genetic features of anaplastic and poorly differentiated thyroid cancer: A single institute experienc."* Oncology letters 15(6), 9174-9182. (2018)

17. Molinaro E., Romei C, Biagini A., Sabini E., Agate L., Mazzeo S., Materazzi G., Sellari-Franceschini S., Ribechini A., Torregrossa L., Basolo F., Vitti P. & Elisei R. *"Anaplastic thyroid carcinoma: from clinicopathology to genetics and advanced therapies"* Nature reviews. Endocrinology 13(11), 644-660. (2017)
18. Bonhomme B., Godbert Y., Perot G., Al Ghuzlan A., Bardet S., Belleannée G., Crinière L., Do Cao C., Fouilloux G., Guyetant S., Kelly A., Leboulleux S., Buffet C., Leteurtre E., Michels JJ., Tissier F., Toubert ME., Wassef M., Pinard C., Hostein I. & Soubeyran I. *"Molecular pathology of anaplastic thyroid carcinomas: A Retrospective Study of 144 Cases"* Thyroid 27(5), 682-692. (2017)
19. Landa I, Ibrahimpasic T, Boucai L, Sinha R, Knauf JA, Shah RH, Dogan S, Ricarte-Filho JC, Krishnamoorthy GP, Xu B, Schultz N, Berger MF, Sander C, Taylor BS, Ghossein R, Ganly I, Fagin JA. "*Genomic and transcriptomic hallmarks of poorly differentiated and anaplastic thyroid cancers*" J Clin Invest.1;126(3):1052-66 (2016)
20. Melo M, Gaspar da Rocha A, Batista R, Vinagre J, Martins MJ, Costa G, Ribeiro C, Carrilho F, Leite V, Lobo C, Cameselle-Teijeiro JM, Cavadas B, Pereira L, Sobrinho-Simões M, Soares P."*TERT, BRAF, and NRAS in Primary Thyroid Cancer and Metastatic Disease*".J Clin Endocrinol Metab. 1;102(6):1898-1907. (2017)
21. Costa AM, Herrero A, Fresno MF, Heymann J, Alvarez JA, Cameselle-Teijeiro J, García-Rostán G. "*BRAF mutation associated with other genetic events identifies a subset of aggressive papillary thyroid carcinoma"*.Clin Endocrinol (Oxf).Apr;68(4):618-34. (2008)
22. **Garcia-Rostan** G, Zhao H, Camp RL, Pollan M, Herrero A, Pardo J, Wu R, Carcangiu ML, Costa J, Tallini G. "*Ras mutations are associated with aggressive tumor phenotypes and poor prognosis in thyroid cancer*". J Clin Oncol. 1;21(17):3226-35. (2003)
23. Insilla AC., Proietti A., Borrelli N., Macerola E., Niccoli C., Vitti P., Miccoli P. & Basolo F. *"TERT promoter mutations and their correlation with BRAF and RAS mutations in a consecutive cohort of 145 thyroid cancer cases."* Oncology letters 15(3), 2763-2770. (2018)